Acta Cryst. (1989). A**45**, 432-441

Standing Waves from a Single Heterostructure on GaAs – a Computer Experiment

BY A. AUTHIER

Laboratoire de Minéralogie-Cristallographie, Universités Paris 6 et 7, associé au CNRS, 4, Place Jussieu, 75252 Paris CEDEX 5, France

J. GRONKOWSKI

Institute of Experimental Physics, University of Warsaw, Hoza 69, Warsaw, Poland

AND C. MALGRANGE

Laboratoire de Minéralogie-Cristallographie, Universités Paris 6 et 7, associé au CNRS, 4, Place Jussieu, 75252 Paris CEDEX 5, France

(*Received* 19 *September* 1988; *accepted* 23 *January* 1989)

Abstract

The phase, node position, intensity and integrated intensity of the standing-wave field have been calculated for a deformed layer on a perfect bulk as a function of angle of incidence and depth inside the crystal. The influence of the various parameters of the deformation, in particular the interface steepness, has been studied. It is found that nodes are never hooked to the deformed planes and that it is only for an incidence corresponding to the middle of the substrate peak that they are hooked to the bulk undeformed planes. The calculation has been applied to two particular situations corresponding to a relatively thick overlayer with an interface of about 100 unit cells, and to very thin overlayers with an interface two unit cells thick. In the latter case it is found that for a surface relaxation of 2% with respect to the bulk the minimum number of lattice planes above the interface for which it can no longer be assumed that the nodes remain hooked to the bulk is of the order of ten.

1. Introduction

Since the pioneering papers by Batterman (1964, 1969) suggesting that standing waves could be used for atom location at crystal surfaces, more than 90 papers, theoretical and experimental, have been published on this topic. Many of the applications of the method have been devoted to the determination of the location of adsorbed surface atoms and of surface reconstruction. But more than a quarter have dealt with the study of deformed or implanted surface layers or of interfaces between substrate and epilayer, for instance interfaces between a silicon substrate and an overlayer of metal silicide. The cases involving a deformed surface layer are important for modern technology and the standing-wave technique is a very promising tool for their study. In none of them can perfect-crystal theory be expected to be rigorously valid. Most authors nevertheless usually assume that, if the epilayer or the surface deformed layer is very thin, the nodes and antinodes remain hooked to the perfect bulk substrate; while only a few authors have taken into account the deformation of the surface layer (Kohn & Kovalchuk, 1981; Kovalchuk, Vartanyantz & Kohn, 1987; Authier, Gronkowski & Malgrange, 1987).

The purpose of this paper is firstly to report the behaviour of nodes and antinodes of standing waves computed by solving Takagi-Taupin equations in a single heterostructure where an epilayer is deposited on a substrate with a continously varying parameter across the interface and to discuss the influence of the steepness of the interface. For practical purposes, the case of an epilayer on a GaAs surface and a 004 reflection has been considered, following the situation studied by X-ray diffractometry by Bensoussan, Malgrange & Sauvage-Simkin (1987).

Secondly, the influence of surface deformation and surface relaxation has been studied. The maximum number of deformed atomic planes for which it can be assumed that the nodes of standing waves remain hooked to the perfect lattice below the deformed layer has been determined.

2. Theoretical considerations

In a perfect crystal, the standing-wave field is given by

$$|D|^2 = |D_0|^2[1 + |\xi|^2 + 2|\xi| \cos(2\pi \mathbf{h} \cdot \mathbf{r} + \psi)] \quad (2.1)$$

where $\xi = |\xi| \exp i\psi = D_h/D_0$ is the ratio of the reflected to the incident amplitude, $\mathbf{h}$ is the reciprocal-lattice vector, oriented towards the inside of the crystal and $\mathbf{r}$ is a position vector. It is well known that $\mathbf{h} \cdot \mathbf{r}$ = constant is the equation of a family of planes parallel to the reflecting planes whose spacing d is the lattice spacing divided by the order of the reflec-

0108-7673/89/060432-10$03.00

tion. The product $\mathbf{h}.\mathbf{r}$ can also be written

$$\mathbf{h}.\mathbf{r} = N + \Delta d/d \tag{2.2}$$

where N is an integer and $\Delta d/d$ is a relative position in the unit cell along the normal to the reflecting planes, oriented towards the inside of the crystal (Fig. 1). Expression (2.1) for the standing-wave field can therefore be written as a function of position within the unit cell,

$$|D|^2 = |D_0|^2[1 + |\xi|^2 + 2|\xi| \cos(2\pi\Delta d/d + \psi)]. \tag{2.3}$$

As the crystal is rocked through the reflection domain from the small- to the large-angle side, the phase ψ varies from $\varphi_h + \pi$ to φ_h, where φ_h is the phase angle of the structure factor, F_h, even in the case of absorbing crystals (Authier, 1986). The nodes of standing waves therefore lie on the planes where the *hkl* Fourier component of the electronic density is maximum on the small-angle side of the reflection domain and progressively drift to a position half way between these planes on the large-angle side.

In a deformed crystal, any point is displaced from the position defined by $\mathbf{r}$ to a position $\mathbf{r}'$ such that

$$\mathbf{r}' = \mathbf{r} + \mathbf{u}(\mathbf{r}) \tag{2.4}$$

where $\mathbf{u}(\mathbf{r})$ is the displacement vector. Equation (2.4) can be rewritten to a close approximation as

$$\mathbf{r} = \mathbf{r}' - \mathbf{u}(\mathbf{r}'). \tag{2.5}$$

Expression (2.1) now becomes, by substitution of (2.5),

$$|D|^2 = |D_0|^2\{1 + |\xi|^2 + 2|\xi| \cos(2\pi\mathbf{h}.[\mathbf{r}' - \mathbf{u}(\mathbf{r}')] + \psi)\} \tag{2.6}$$

where D, D_0, ξ and ψ are now position dependent.

The equation of the deformed planes is

$$\mathbf{h}.\mathbf{r}' - \mathbf{h}.\mathbf{u}(\mathbf{r}') = N, \tag{2.7}$$

the origin being taken on a lattice plane. It can also be written

$$\mathbf{h}'.\mathbf{r}' = N \tag{2.8}$$

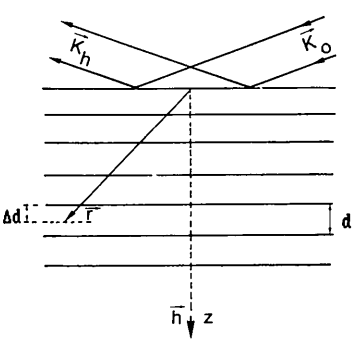

Fig. 1. Geometry of crystal lattice planes.

where $\mathbf{h}' = \mathbf{h} + \delta\mathbf{h} = \mathbf{h} - \nabla(\mathbf{h}.\mathbf{u})$ is the local reciprocal-lattice vector (Authier, 1966).

Any point in the crystal defined by a position vector $\mathbf{r}'$ is now characterized by its relative position $\Delta d'/d'$ relative to the deformed planes:

$$\mathbf{h}'.\mathbf{r}' = \mathbf{h}.\mathbf{r}' - \mathbf{h}.\mathbf{u}(\mathbf{r}') = N + \Delta d'/d' \tag{2.9}$$

and (2.3) for the standing-wave field still holds but it is calculated at a position relative to the deformed cell and D, D_0, ξ and ψ are position dependent. We shall limit ourselves in this paper to the case where $\mathbf{u}(\mathbf{r})$ depends only on the depth z below the crystal surface. If we introduce the dimensionless deviation parameter η of the incident wave, usual in dynamical theory and related to the departure from Bragg's angle of this incident wave (*e.g.* Authier, 1986), (2.3) becomes

$$|D(\eta, z)|^2 = |D_0(\eta, z)|^2\{1 + |\xi(\eta, z)|^2 + 2|\xi(\eta, z)| \cos[2\pi(\Delta d'/d') + \psi(\eta, z)]\}. \tag{2.10}$$

Here, η stands for the real part of the deviation parameter, which is the only one which will be considered. The origin is taken at the middle of the Bragg peak for the substrate ($\eta_s = 0$).

It is also possible to relate the same position to the planes before deformation. Let us call this relative position $\Delta d_s/d_s$. If $\Delta d'/d'$ corresponds to a particular atomic site in the unit cell, it is constant in the whole heterostructure and $\Delta d_s/d_s$ is depth dependent. The two relative positions are related by

$$\Delta d'/d' = \Delta d_s/d_s(z) - \mathbf{h}.\mathbf{u}(z). \tag{2.11}$$

If we consider an epilayer or a deformed layer on a perfect bulk, the assumption usually made that the nodes remain hooked to the substrate, that is that their spacing remains constant throughout the whole depth, implies that the value of the standing-wave field would be given by

$$|D(\eta, z)|^2 = |D_{0s}(\eta)|^2\{1 + |\xi_s(\eta)|^2 + 2|\xi_s(\eta)| \cos[2\pi\Delta d_s/d_s(z) + \psi_s(\eta)]\} \tag{2.12}$$

where $D_{0s}(\eta)$, $\xi_s(\eta)$ and $\psi_s(\eta)$ are the solutions of dynamical theory for the perfect substrate and $\Delta d_s/d_s$ represents the relative position with respect to the substrate planes in the bulk.

The important question for the interpretation of standing-wave experimental results is the behaviour of the nodes. Comparison of (2.10) and (2.12) shows that they only remain hooked to the undeformed substrate planes if

$$2\pi\Delta d'/d' + \psi(\eta, z) = 2\pi\Delta d_s(z)/d_s + \psi_s(\eta); \tag{2.13}$$

that is, using (2.11), if

$$\psi(\eta, z) - \psi_s(\eta) = 2\pi\mathbf{h}.\mathbf{u}(z). \tag{2.14}$$

On the other hand, if $\psi(\eta, z)$ is *not* depth dependent, the node spacing is continuously equal to that of the local reflecting planes and the nodes are therefore hooked to the deformed planes.

Generally speaking, it is the depth variations of the phase $\psi(\eta, z)$ which command the variations of the node spacing and the drift of the node positions relative to the substrate or to the deformed planes.

The phase and amplitude of the incident and reflected waves were calculated by solving Takagi–Taupin equations (Takagi, 1962, 1969; Taupin, 1964) using the varying-step algorithm described by Bensoussan *et al.* (1987), working up towards the surface from a depth at which the crystal can be assumed to be perfect. The variations of the standing-wave field with angle of incidence of the incident wave have been calculated for any depth inside the crystal and for any atomic position within the unit cell. The relative position of the standing-wave field will always be given, unless otherwise stated, with respect to the deformed planes, since this is what is physically significant.

It is a property of Takagi–Taupin equations in the Bragg case that since the solution is calculated by integrating from the bottom up towards the crystal surface, the solution at a certain depth is independent of the strain distribution above it (Taupin, 1964).

In standing-wave experiments, there are two quantities of importance, namely the field at the surface or along a given plane inside the crystal if it is an impurity which is being investigated and the integrated field over a certain crystal thickness if it is the signal, fluorescent yield or photoemission, from the crystal itself. The integrated field has therefore also been calculated. This is performed working down from the surface. The integration depth, which can be controlled experimentally, has been chosen here arbitrarily to be equal to half an extinction distance.

3. Elastic model of the strain distribution

The reflecting planes are taken to be parallel to the surface and the displacement vector is normal to that surface. The depth dependence of the strain has been taken to be

$$\mathrm{d}u(z)/\mathrm{d}z = -(\Delta a/a)\{1+\exp[(z-z_I)/C]\}^{-1} \quad (3.1)$$

following Bensoussan *et al.* (1987). The z origin is taken at the surface and z increases towards the inside of the crystal; if the epilayer lattice parameter is larger than the substrate one, $\mathrm{d}u/\mathrm{d}z$ is taken negative by convention.

Expression (3.1) describes a heterostructure with an epilayer of parameter $a+\Delta a$ on a substrate of lattice parameter a. The interface is characterized by its midposition, z_I, and its steepness by C (Fig. 2). The relative lattice-parameter variation $\Delta a/a$, which is also equal to the relative variation in reflecting-plane spacing, $\Delta d/d$, is related to the difference $\Delta\theta$ in Bragg angle between epilayer and substrate by differentiation of Bragg's law:

$$\Delta a/a = \Delta d/d = -\Delta\theta/\tan\theta. \quad (3.2)$$

Introducing the variation $\Delta\eta$ of the deviation parameter which is proportional to $\Delta\theta$, since we have assumed the reflection to be symmetrical, we can also write (3.2) as

$$h\Delta d/d = -\Delta\eta/\Lambda \quad (3.3)$$

where Λ is the extinction distance. In the integration of the Takagi–Taupin equations, it is $h\,\mathrm{d}u/\mathrm{d}z$ which intervenes. From (3.1) and (3.3), it is equal to

$$h\,\mathrm{d}u/\mathrm{d}z = (\Delta\eta/\Lambda)\{1+\exp[(Z-1)/c]\}^{-1} \quad (3.4)$$

where $Z = z/z_I$ and $c = C/z_I$ are reduced parameters and the reciprocal-lattice vector **h** is oriented towards the inside of the crystal.

The absolute total displacement $u(z)$ with respect to the perfect lattice is obtained by integrating (3.1) between the depth where the crystal substrate can be assumed to be perfect and depth z and

$$hu(z) = cZ_I\Delta\eta((1-Z)/2c + \log\{2\cosh[(1-Z)/2c]\}) \quad (3.5)$$

where $Z_I = z_I/\Lambda$. Use of the reduced parameters Z, Z_I, c and $\Delta\eta$ enables one to get general results applicable to any particular crystal.

In order to simulate a deformed surface layer, one can simply use the same model by putting the surface of the crystal at a position close to $z = z_I$.

On the other hand, if one considers an epilayer where the lattice parameter has practically reached

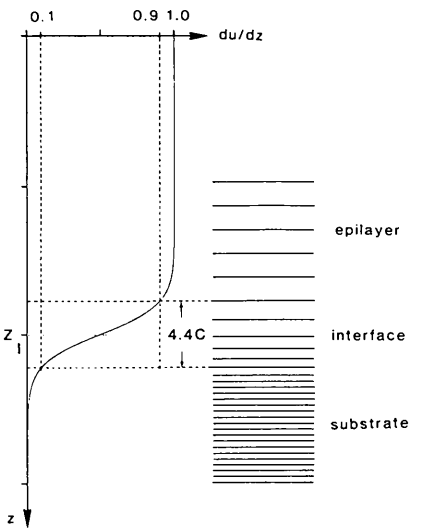

Fig. 2. Elastic model of the strain distribution in the heterostructure. The value of the strain varies from 0·1 to 0·9 $\Delta a/a$ in a depth range $\mp 2{\cdot}2\,C$ around the middle of the interface at depth z_I.

the value $a+\Delta a$, the depth z at which $u(z)$ is calculated is well above the middle of the interface, $z_I (z \ll z_I)$, and (3.5) reduces to

$$hu(z) = Z_I(1-Z)\Delta\eta. \qquad (3.6)$$

The total displacement $u(z)$ at depth z is equal to the parameter mismatch, Δa, times the number of lattice planes above the middle of the interface, $(z_I - z)/a$.

It will be noted that (3.6) does not depend on C. In other words, when the epilayer is much thicker than the interface width, the integrated displacement does not depend on the interface steepness. In particular, at the surface ($Z=0$)

$$hu(0) = Z_I\Delta\eta = (z_I/d)(\Delta a/a). \qquad (3.7)$$

4. Standing-wave field and phase in the case of an epilayer

4.1. *Experimental conditions*

Diffraction conditions: 004 reflection, Cu $K\alpha$. Substrate: (001) GaAs; Bragg angle 33·03°; extinction distance $\Lambda = 5{\cdot}01$ μm; absorption depth 15·9 μm; half-height width 7·3″. Epilayer thickness: $z_I = 1{\cdot}31$ μm ($Z_I = 0{\cdot}26$); relative lattice-parameter change: $\Delta a/a = +7{\cdot}8\times10^{-4}$ ($\Delta\theta = 101''$, $\Delta\eta = -27{\cdot}7$). Interface thickness: $C = 0{\cdot}05$ μm ($c = 0{\cdot}038$).

The surface of the heterostructure has been considered to be at $z=0$. The value (3.7) of $hu(0)$ at the surface is equal to $-7{\cdot}2$.

4.2. *Results*

4.2.1. *Rocking curve.* Fig. 3 shows the variations with angle of incidence of the reflected intensity at the surface. The rocking curve presents the epilayer and substrate peaks, with fringes in between, as is well known. The angle between the epilayer and substrate peaks is proportional to the parameter mismatch (3.2) and the period of the fringes is inversely proportional to the thickness of the epilayer. It is equal to that of the fringes which would be observed for a thin perfect crystal of the same thickness as that of the epilayer.

Fig. 4 represents in a pseudo-three-dimensional way how the rocking curve varies with depth: rocking curves at increasing depths are plotted on the same diagram. As mentioned above, each of the rocking curves is identical to what it would be if the surface of the crystal was at the corresponding depth. It can be noted that the distance of the epilayer to substrate peaks decreases to zero at the interface.

4.2.2. *Standing-wave field.* Fig. 5 shows the variations with angle of incidence of the standing-wave field at the surface for two positions in the unit cell, as well as the rocking curve. The two positions are situated along the reflecting planes and half way between them. It can be seen that there are oscillations around the positions of the epilayer and substrate peaks and in between, as in the case of the rocking curve, and with the same periodicity. The fringes for the two positions in the unit cell are out of phase by half a fringe, as is to be expected, and, more generally, the shape of the signal is quite different and easily distinguishable for the two positions. In a real experiment, the signal would be convoluted with the experimental width of the beam coming from the monochromator, which would result in a damping of the

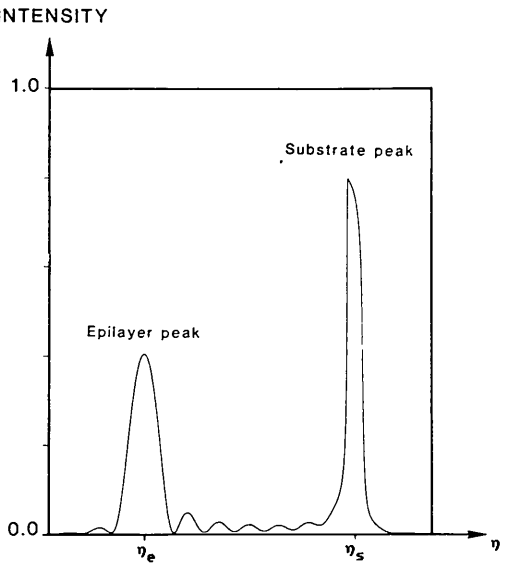

Fig. 3. Rocking curve of the heterostructure: $|D_h|^2/|D_0|^2$. The middle of the Bragg peaks for the epilayer and the substrate corresponds to values η_e and η_s of the deviation parameter, respectively.

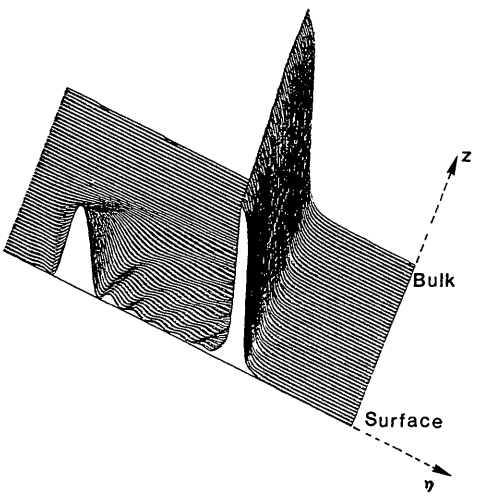

Fig. 4. Pseudo-three-dimensional representation of the reflected intensity at various depths between the crystal surface and the bulk.

fringes. The shape of the signal around the epilayer peak is very similar to that observed for a thin crystal of the same thickness as the epilayer (Authier, 1987), but with a slightly different fringe spacing. However, the period of the fringes between the peaks is exactly identical to that in the corresponding perfect thin crystal.

The standing-wave field integrated over a thickness equal to half an extinction distance, that is, in the present case, to nearly twice that of the epilayer, is represented in Fig. 6. The field is represented for the same two positions in the unit cell as in Fig. 5 and corresponds to the yield from the crystal itself. The oscillations are damped out. The signal around the substrate peak is very close to that which would be emitted by the perfect crystal and gives no information about the epilayer, but that around the epilayer peak is characteristic of the heterostructure and enables the determination of atomic positions in the epilayer.

Fig. 7 represents in the same pseudo-three-dimensional way as Fig. 4 the variations of the standing-wave field with depth. As for the rocking curve,

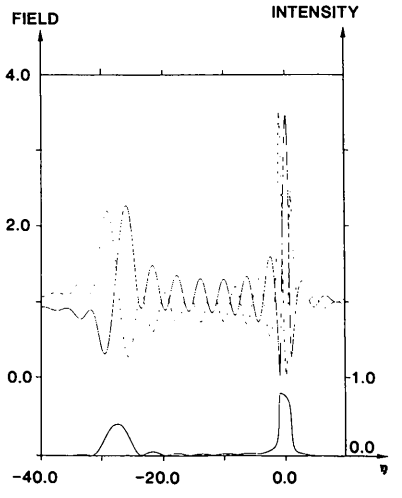

Fig. 5. Upper curves: standing-wave field $|D(\eta)|^2/|D_0|^2$ at the surface. Solid curve: $\Delta d'/d' = 0{\cdot}0$; dashed curve: $\Delta d'/d' = 0{\cdot}5$. Lower solid curve: rocking curve.

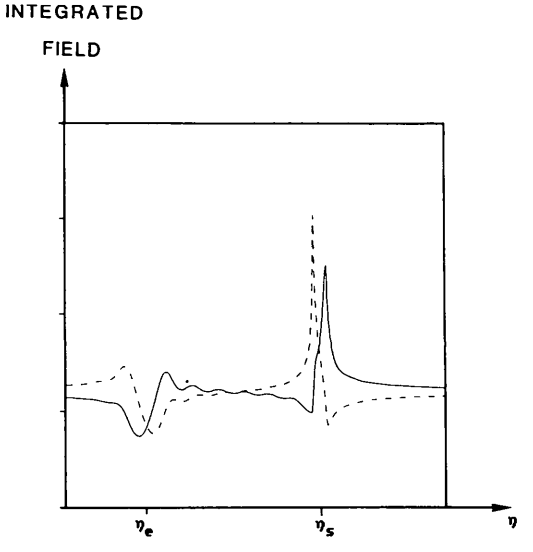

Fig. 6. Integrated standing-wave field (arbitrary units); solid curve: $\Delta d'/d' = 0{\cdot}0$; dashed curve: $\Delta d'/d' = 0{\cdot}5$. The integration has been performed over a depth equal to half an extinction distance, that is, in this case, to about twice the thickness of the epilayer.

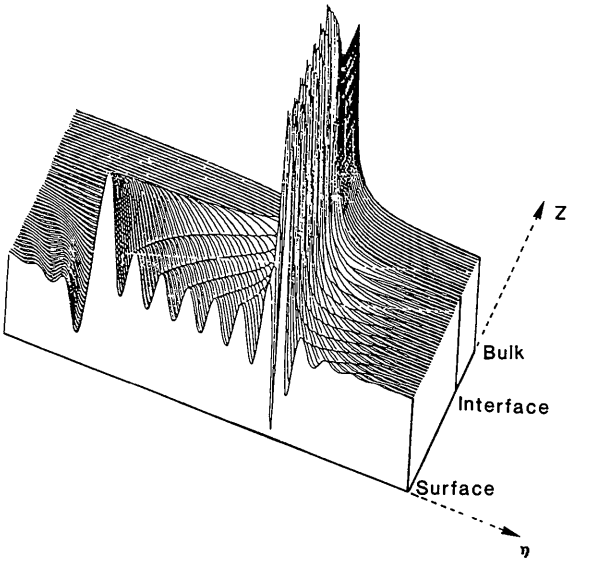

Fig. 7. Pseudo-three-dimensional representation of the standing-wave field $|D(\eta, z)|^2$ at various depths between the surface and the bulk. $\Delta d'/d' = 0{\cdot}0$.

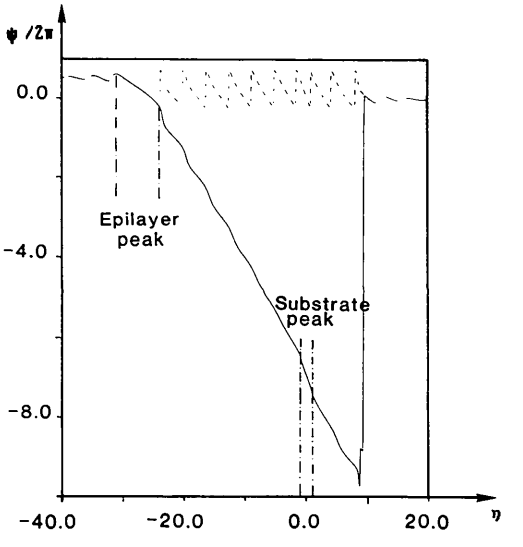

Fig. 8. Variations with the deviation parameter of the phase, $\psi(\eta, 0)$, at the surface. Dashed curve: value modulo 2π; solid curve: total value.

the fringe spacing decreases as depth increases, following the decrease of the distance between the epilayer and substrate signals until it is equal to zero at the interface.

4.2.3. *Phase.* Fig. 8 represents the variations with angle of incidence of the phase ψ of the ratio ξ of the complex amplitudes of the two waves in the wave field, D_h/D_0, calculated at the surface of the crystal and given in units of 2π. Two representations of the same curve are plotted in this figure. The dashed curve corresponds to the variations of the phase modulo 2π. The periodic jumps show that between the substrate and the epilayer peaks the phase varies by an amount somewhat larger than 2π and the full curve represents these total variations which correspond to the adaptation of the wave fields to the change in lattice parameter between substrate and epilayer. It has been checked that the period of the standing-wave fringes, and therefore that of the rocking curve, corresponds exactly to the range in η over which the phase varies by 2π.

Fig. 9 gives the three-dimensional view of the total variations of the phase with depth. The top and bottom curves of this diagram are plotted in Fig. 10. They represent the variations of the phase in the bulk below the interface and at the surface. These figures show that:

(*a*) The variations of the phase with angle of incidence in the bulk are identical to what they are in the perfect thick crystal case, as they should be.

(*b*) The phase at the surface at the centre of the epilayer peak, $\psi(\eta_e, 0)$, is equal to $\pi/2$ and to the phase in the bulk at the centre of the substrate peak, $\psi(\eta_s, \infty)$.

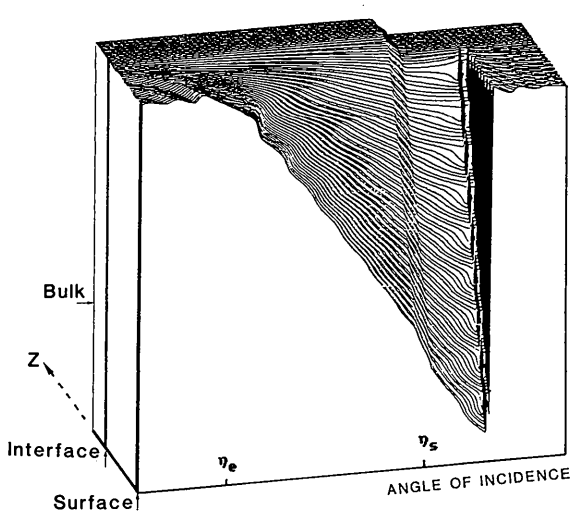

Fig. 9. Pseudo-three-dimensional representation of the phase $\psi(\eta, z)$ at various depths between the surface and the bulk. The epilayer peak around η_e and the substrate peak around η_s can be observed.

(*c*) The phase is strongly depth dependent in the angular range from the epilayer peak up to a critical value, η_c, lying further than the substrate peak.

(*d*) In particular, it is found that the difference in phase at the substrate Bragg peak, η_s, between the surface and the bulk, which is equal to the phase difference at the surface between the epilayer and substrate Bragg positions,

$$\Delta\psi(\eta) = \psi_s(\eta_s) - \psi(\eta_s, 0) = \psi(\eta_e, 0) - \psi(\eta_s, 0) \quad (4.1)$$

is equal to $7{\cdot}2 \times 2\pi$, that is to the value of $-2\pi hu(0)$ calculated in § 4.1. This result combined with (3.7) shows that the average slope $\Delta\psi/\Delta\eta$ of the variations of the phase on the full curve of Fig. 8 ($\Delta\eta = \eta_e - \eta_s$) is equal to $-2\pi Z_I$ and that the average period of the fringes of the dashed curve on the same curve is equal to $1/Z_I$, that is to the period of the fringes for a

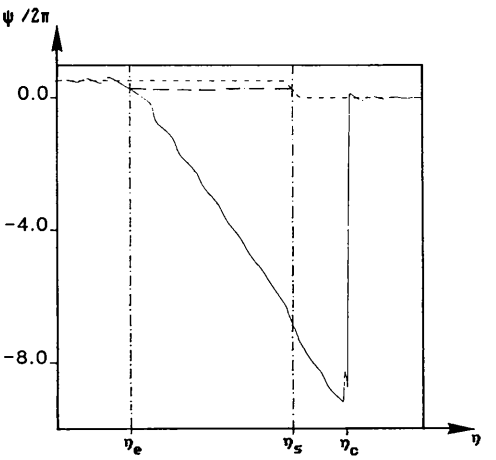

Fig. 10. Dashed curve: $\psi(\eta, \infty)$, phase in the bulk; solid curve: $\psi(\eta, 0)$, phase at the surface. The Bragg positions for the epilayer and substrate peaks are indicated by broken vertical lines.

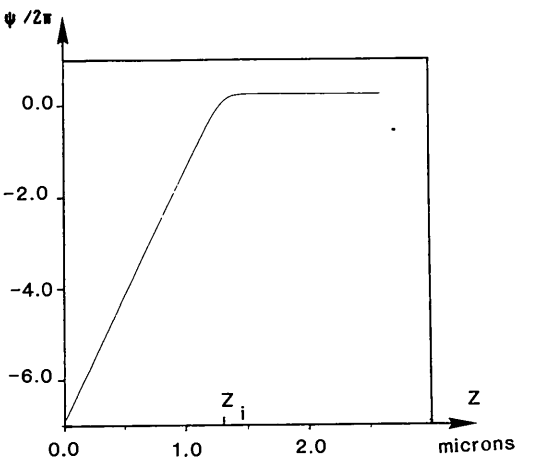

Fig. 11. $\psi(\eta_s, z)$, depth dependence of the phase at the Bragg position for the substrate. The curve obtained for $hu(z)$ is identical.

perfect thin crystal of the same thickness, Z_l, as the epilayer.

Furthermore, it can be shown that the variations (3.6) of $hu(z)$ can be rigorously superimposed on those of $\psi(\eta_s, z)$ given in Fig. 11. This means that condition (2.14) is satisfied for the substrate Bragg position and this very important result will be interpreted in the next section.

(*e*) At the middle of the epilayer Bragg peak, the phase difference between the bulk and the surface is equal to $\pi/2$.

(*f*) There is *no* value of the deviation parameter for which the phase is rigorously independent of the depth. However, the variations are very small for values smaller than the epilayer Bragg peak and for values larger than the critical value η_c.

4.2.4. *Discussion*; *position of the nodes.* In the deformed crystal considered in this paper, there is no curvature of the reflecting planes. Only their lattice spacing is changed and their positions are displaced with respect to these which they would occupy in the perfect substrate. As described in § 3, the epilayer has a lattice parameter larger than that of the bulk and the displacement of the deformed planes with respect to the perfect ones increases as one considers planes further away from the bulk and closer to the surface. As has been said in § 2, the relative position of the nodes of standing waves with respect to the deformed and undeformed lattice planes is determined by the value of the phase. If the phase is *not* depth dependent, the nodes are hooked to the deformed planes; if condition (2.14) is satisfied, they are hooked to the substrate. In all other cases, they drift with respect to these positions. More accurately, the depth dependence of the phase at a given value of the deviation parameter η shows that the depth dependence of the node spacing is different from that of the deformed lattice planes. Quantitatively, and with the variation of $\psi(\eta, 0)$ approximated by a straight line of slope $-2\pi Z_l$ between η_e and η_c, the phase difference at a given η between the bulk and the surface gives by analogy with (3.7) the relative difference $\Delta d_n/d_n$ between the node spacing and the reflecting plane spacing at the surface as

$$\Delta d_n/d_n = (d/2\pi z_l)[\psi(\eta, \infty) - \psi(\eta, 0)]. \quad (4.2)$$

The analysis of § 4.2.3 can therefore immediately be translated in terms of node positions. The fact that condition (2.14) is satisfied for one angle of incidence only shows that it is only for the middle of the substrate Bragg peak, η_s, that the nodes remain hooked to the undeformed lattice planes in the bulk. It is easy to check with (4.2) that $\Delta d_n/d_n$ is then indeed equal to $\Delta d_s/d_s(0)$. For all other angles of incidence there is a drift of the nodes with respect to the substrate planes.

When the crystal is rotated towards angles of incidence larger than the substrate Bragg angle in the range $\eta_s < \eta < \eta_c$, the nodes lag behind the substrate planes. In other words, as $|\psi(\eta, \infty) - \psi(\eta, 0)|$ becomes larger than $2\pi|hu(0)|$, the node spacing becomes decreasingly smaller than that of the substrate lattice planes. At $\eta = \eta_c$, for instance, (4.2) shows that the relative difference between the node spacing and the bulk lattice spacing is equal to $-2{\cdot}5 \times 10^{-4}$. The standing waves, however, remain coupled to them in a certain way. As the angle of incidence increases further away from the substrate peak, the amplitude of the field becomes very small and, at the critical value, η_c, of the deviation parameter, the coupling of the standing waves with the substrate becomes so weak that they completely unhook; the node spacing in the epilayer suddenly starts increasing very fast until it nearly catches up with that of the deformed planes around which it oscillates.

When the crystal is rotated from the substrate Bragg peak towards the epilayer Bragg peak ($\eta_e < \eta < \eta_s$), the node spacing becomes larger than that of the substrate and the nodes drift from the substrate lattice positions towards the epilayer ones, but not enough to catch up with them.

At the Bragg position for the epilayer, the nodes move nearly in phase with the deformed planes, but with a drift of $\pi/2$ between the bottom and the top of the epilayer. For angles of incidence smaller than the epilayer Bragg angle, the nodes oscillate around the deformed planes. They are therefore *never* exactly hooked to the deformed planes.

4.2.5. *Influence of interface steepness.* The influence of interface steepness characterized by C is shown in Figs. 12 to 14. Values of C ranging from 0·005 to 0·5 μm have been considered. The former corresponds to about ten lattice planes (the lattice parameter of GaAs has been taken to be equal to 5·6532 Å) and to a relatively steep interface (steeper interfaces will be discussed in § 5), the upper part of the epilayer being practically perfect. In the latter case, C corresponds to about 1000 lattice planes, which is a relatively large fraction of the epilayer thickness; the lattice spacing in the epilayer is always far from being constant and this case simulates the behaviour of standing waves in a continuously deformed crystal.

Three main effects may be observed on the figures:

(*a*) The amplitudes of the fringes of the phase (Fig. 12), the field (Figs. 13*a* and *b*) and the integrated field (Fig. 14) are much larger *outside* the range $\eta_e < \eta < \eta_s$ for the steeper interfaces and *inside* this range for the broader interfaces.

(*b*) The angular position of the integrated signal from the epilayer depends strongly on the shape of the interface, in particular for broad interfaces. It is much less so for steep interfaces. By contrast, the position of the signal from the substrate peak

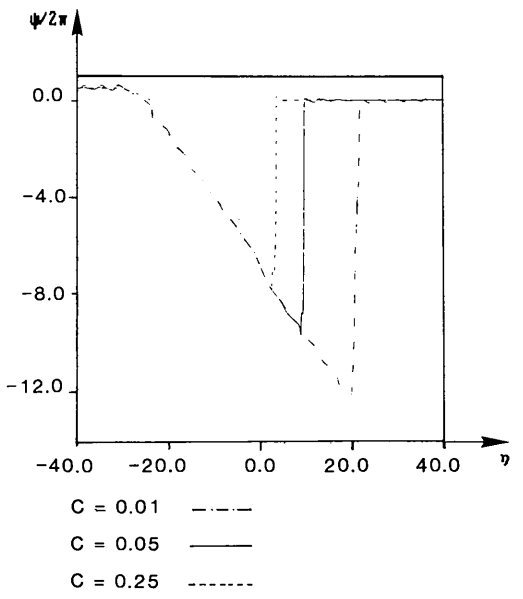

Fig. 12. Influence of interface steepness on the phase $\psi(\eta, 0)$. The values of C are given in micrometres.

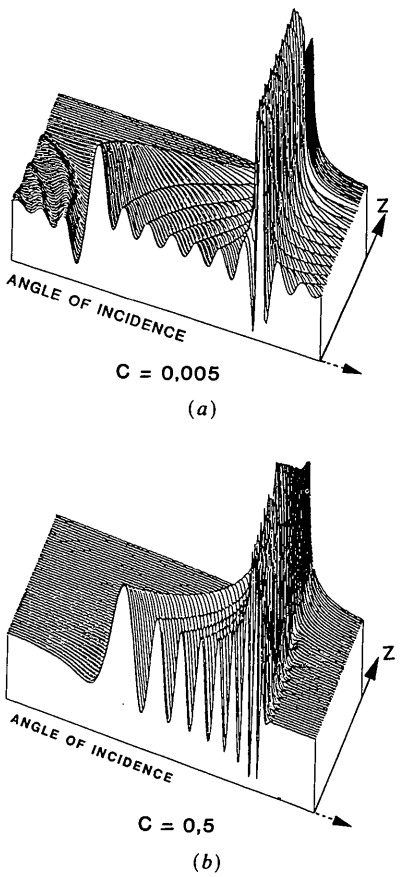

Fig. 13. Influence of interface steepness on the standing-wave field $|D(\eta, 0)|^2$ at the surface for $\mathbf{h}.\mathbf{r} = 0{\cdot}0$. (*a*) $C = 0{\cdot}005$ μm; (*b*) $C = 0{\cdot}5$ μm.

practically does not depend on the shape of the interface.

(*c*) the critical value, η_c, of the deviation parameter for which the standing waves uncouple from the substrate and the corresponding value of the phase are very strongly dependent on interface steepness (Fig. 12). The values of the phase at $\eta = \eta_e$ and $\eta = \eta_s$ are however the same for all the curves since they do not depend on C and it is possible to use (4.2) to evaluate the node spacing at $\eta = \eta_c$ for the different values of C. For instance, the relative difference between the node spacing at the surface and the perfect reflecting plane spacing in the bulk is of the order of $-0{\cdot}2 \times 10^{-4}$, $-2{\cdot}5 \times 10^{-4}$ and $-4{\cdot}8 \times 10^{-4}$ for $C = 0{\cdot}25$, $0{\cdot}05$ and $0{\cdot}01$ μm respectively.

5. Deformed surface layer

5.1. *Experimental conditions*

In this section we consider the same diffraction conditions as in § 4 and the same strain distribution (3.1). But in order to simulate a surface relaxation, the following parameters of the deformation have been chosen:

$\Delta a/a = +2\%$, which corresponds to $\Delta\eta = -709{\cdot}5$;

$z_I = 1{\cdot}000$ μm

$C = 1{\cdot}4133$ Å $= a/4$ $(c = 0{\cdot}00014133)$.

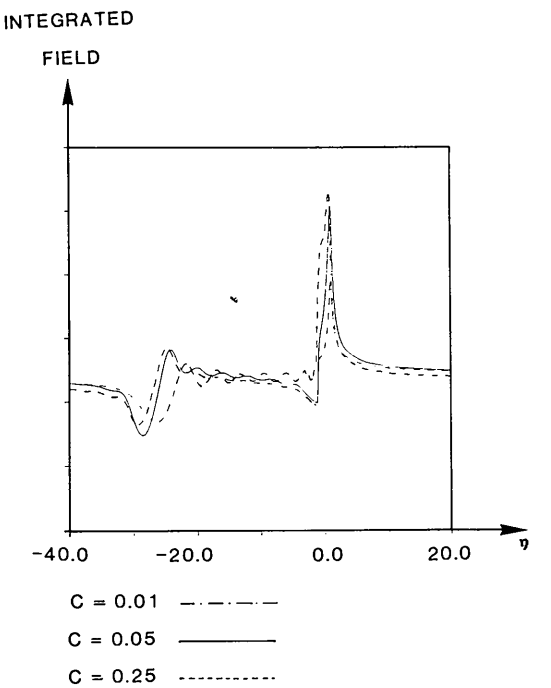

Fig. 14. Influence of interface steepness on the integrated standing-wave field for $\mathbf{h}.\mathbf{r} = 0{\cdot}0$. The integration depth is equal to half an extinction distance. Values of C are given in micrometres.

Table 1. *Variations of lattice parameter and of $hu(z)$ with depth*

$z - z_I$	$\Delta a/a$ (%)	$hu(z)$
a	0·04	0·000
$a/2$	0·24	0·000
0	1·00	−0·014
$-a/2$	1·76	−0·043
$-a$	1·96	−0·080
$-2a$	2·00	−0·160
$-3a$	2·00	−0·240
$-4a$	2·00	−0·320
$-5a$	2·00	−0·400
$-6a$	2·00	−0·480
$-7a$	2·00	−0·560
$-8a$	2·00	−0·640
$-9a$	2·00	−0·720
$-10a$	2·00	−0·800

Table 1 gives the corresponding values of the lattice-parameter varitions and of $hu(z)$ at various depths close to $z = z_I$. It can be seen that the lattice-parameter relaxation is equal to 1·92% over two unit cells. A surface relaxation over a few unit cells has thus been simulated.

As has been said in § 2, the crystal surface can be put at any level defined by a given value of z. The value of z_I is only one of the parameters used in (3.1) to define the strain distribution. In § 4, the crystal surface was put at $z = 0$ for convenience. Here the properties of the standing waves will be studied assuming the crystal surface to be put at any of the levels defined by the values of z given in Table 1. It must be stressed that the model does not pretend to be elastically the most stable description of the surface. It is simply used as an analytical representation of a surface relaxation in order to find out whether the nodes remain hooked to the substrate or not. The general result is expected to hold also for any other elastic model.

5.2. *Results*

Fig. 15 shows the variations with angle of incidence of the standing-wave field along the lattice planes at $z = z_I$ and at each of the ten successive layers above it. They were calculated putting $\Delta d'/d' = 0$ in (2.10). If, on the other hand, one assumes condition (2.14) to be satisfied, that is that the nodes remain hooked to the substrate, it is possible to calculate the field by means of (2.12) where $\Delta d_s/d_s(z)$ is put equal to each of the successive values (2.11) of $hu(z)$ given in Table 1. It is found that for the first few levels above z_I the resulting curves superimpose quite well with those of Fig. 15 but that they start deviating around the seventh plane. The first one which deviates significantly is the one at $z = z_I - 10a$. The two corresponding curves, calculated by means of (2.10) and (2.12), respectively, are plotted in Fig. 16. The error in the atomic position made when assuming the nodes to be hooked to the substrate is of the order of 0·01 lattice spacing. This error cannot be determined accurately as the shape of the curve calculated using Takagi-Taupin equations cannot be matched exactly using perfect-crystal theory. Only a best fit can be found.

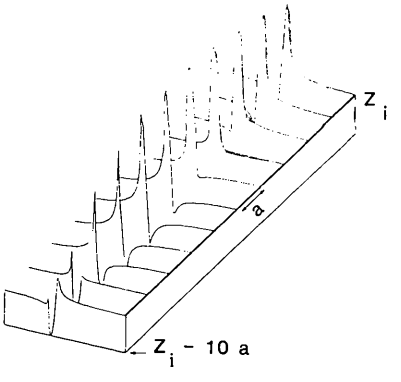

Fig. 15. Standing-wave field at ten successive atomic layers above the middle of the interface. The surface relaxation is equal to 2% and takes place over one unit cell on each side of $z = z_I$.

The same study has been repeated for different values of the parameters of the strain distribution and the conclusion is roughly the same in all cases. When there is a coherent thin overlayer on a perfect bulk, the parameter misfit being a few percent and the interface one or two unit cells thick, the position of the planes of the overlayer can only be deduced with accuracy from standing-wave results with the hooked-nodes approximation for at most the first ten or so layers.

6. Concluding remarks

The main results of the computer simulation described in this paper are summarized below.

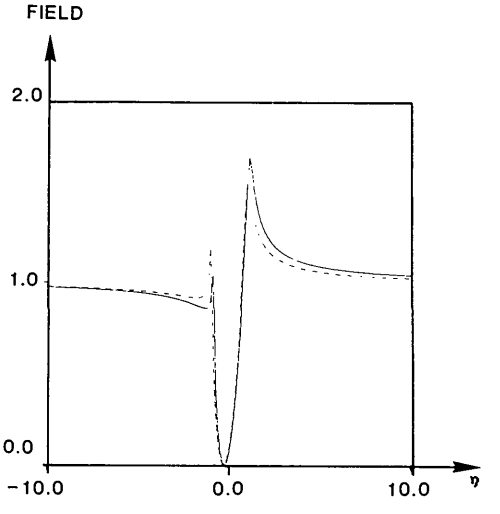

Fig. 16. Solid curve: standing-wave field at $z = z_I - 10a$, from Fig. 15, calculated by solving Takagi-Taupin equations. Dashed curve: standing-wave field calculated assuming nodes to be hooked to the substrate and at a position in the unit cell corresponding to the atomic displacement $hu(z)$ at $z = z_I - 10a$.

When a crystal surface is deformed, the standing waves can only be assumed to be hooked to the perfect bulk lattice planes for the first ten or so atomic layers at any angle of incidence, but are hooked throughout the whole thickness at the exact Bragg angle for the substrate. In all other cases the node spacing depth distribution is different from either that of the bulk or that of the deformed crystal. Great caution should therefore be taken in interpreting standing-wave results of crystals with a deformed surface layer or an overlayer with a slightly different lattice parameter.

If, however, an appropriate elastic model describing the strain distribution in the deformed crystal is known, the exact position of the nodes can be deduced from the phase distribution $\psi(\eta, z)$ and the standing-wave field calculated. By comparing the results with experimental measurements it is then possible to determine atom location at the surface or inside the deformed layer, as in the perfect-crystal case. The amount of strain in the epilayer of a heterostructure can be determined as has been shown by Koval'chuk *et al.* (1987) and the steepness of the interface estimated.

This work was partly supported by CNRS-ATP project 172 and by grant CPBP 01.05 (Warsaw).

References

AUTHIER, A. (1966). *J. Phys. Radium*, **27**, 57-60.
AUTHIER, A. (1986). *Acta Cryst.* A**42**, 414-426.
AUTHUER, A. (1987). *Acta Cryst.* A**43**, C216.
AUTHIER, A., GRONKOWSKI, J. & MALGRANGE, C. (1987). *Acta Cryst.* A**43**, C217.
BATTERMAN, B. W. (1964). *Phys. Rev. A*, **133**, 759-764.
BATTERMAN, B. W. (1969). *Phys. Rev. Lett.* **22**, 703-705.
BENSOUSSAN, S., MALGRANGE, C. & SAUVAGE-SIMKIN, M. (1987). *J. Appl. Cryst.* **20** 222-229.
KOHN, V. G. & KOVAL'CHUK, M. V. (1981). *Phys. Status Solidi A*, **64**, 359-366.
KOVAL'CHUK, M. V., VARTANYANTZ, I. A. & KOHN, V. G. (1987). *Acta Cryst.* A**43**, 180-187.
TAKAGI, S. (1962). *Acta Cryst.* **15**, 1311-1312.
TAKAGI, S. (1969). *J. Phys. Soc. Jpn*, **27**, 1239-1253.
TAUPIN, D. (1964). *Bull. Soc. Fr. Minéral. Cristallogr.* **87**, 469-511.

SHORT COMMUNICATIONS

Contributions intended for publication under this heading should be expressly so marked; they should not exceed about 1000 *words; they should be forwarded in the usual way to the appropriate Co-editor; they will be published as speedily as possible.*

Acta Cryst. (1989). A**45**, 441-443

Direct methods and structures showing superstructure effects. V. The use of one-phase seminvariants and quartet invariants.

By G. CASCARANO and C. GIACOVAZZO, *Dipartimento Geomineralogico, Università, Campus Universitario, Via Amendola,* 70124 *Bari, Italy,* M. LUIĆ, *Institut 'Rudjer Bošković', Bijenička* 54, 41000 *Zagreb, Yugoslavia* and I. VICKOVIĆ, *Zavod za Opću i Anorgansku Kemiju, Prirodoslovno-Matematički Fakultet, Sveučilište, ul. Soc. Revolucije* 8, 41000 *Zagreb, Yugoslavia*

(*Received* 16 *May* 1988; *accepted* 3 *January* 1989)

Abstract

Figures of merit based on PSI0 and on strong triplets are often unreliable for structures with superstructure effects. Prior information on pseudotranslational symmetry is used in order to estimate one-phase seminvariants. These are used, together with quartet invariants, for finding the correct solution in a multisolution process.

Symbols and abbreviations

Papers by Cascarano, Giacovazzo & Luić (1988*a*, *b*) will be denoted respectively as papers III and IV.
s.s.: structure seminvariant.
s.i.: structure invariant.
Other symbols as in paper III.

Introduction

Different probabilistic approaches are today available for estimating triplet invariants in crystal structures with superstructure effects (Böhme, 1982, 1983; Fan Hai-fu, Yao Jiaxing, Main & Woolfson, 1983; Gramlich, 1984; Cascarano, Giacovazzo & Luić, 1985, 1987, 1988*a*, *b*). No attempt has so far been made for estimating (in a probabilistic sense) other types of s.i.'s or s.s.'s, even if their role in this kind of structure is expected to be non-negligible.

Default runs of the *SIR* package (Cascarano, Giacovazzo, Burla, Nunzi, Polidori, Camalli, Spagna & Viterbo, 1985) involve, besides triplets, also quartet invariants and one- and two-phase seminvariants. However, only triplets are used for structures with superstructure effects according to papers III and IV. Even if they are successful in solving such structures, corresponding figures of merit (FOM's) for finding the correct solution are usually unsatisfactory (Cascarano, Giacovazzo & Viterbo, 1987). Two FOM's involving triplets (ALFCOMB and PSCOMB) are used in *SIR*, both based on the agreement between the theoretical and the experimental distributions of the α parameter for strong and PSI0 triplets respectively: the best agreement is characterized by unitary values of ALFCOMB

0108-7673/89/060441-03$03.00